International Journal of Marine Energy 10 (2015) 52–69

Contents lists available at ScienceDirect

International Journal of Marine Energy

journal homepage: www.elsevier.com/locate/ijome

Perspective on the risk that sediment-laden ice poses to in-stream tidal turbines in Minas Passage, Bay of Fundy

Brian G. Sanderson *, Anna M. Redden

Acadia Center for Estuarine Research, Acadia University, Nova Scotia, Canada

ARTICLE INFO

Article history:
Received 2 December 2013
Revised 15 January 2015
Accepted 23 January 2015
Available online 4 February 2015

Keywords:
Subsurface
Ice
Buoyancy
Turbine
Tide

ABSTRACT

Large sediment-laden ice cakes form in the Minas Basin and concern has been raised that they might pose a substantial danger to in-stream tidal turbines deployed in strong tides of Minas Passage, Bay of Fundy. Consideration of buoyancy and drag shows that large ice cakes must have density within a much more narrow range than small ice cakes if they are to be dragged below the surface by turbulent motion. Density measurements of ice samples cut from large ice cakes show a bimodal distribution, with most samples being clearly buoyant and a minority being clearly negatively buoyant. Ice cakes are composed from materials (sediment, ice, salt, air) that are all substantially different in density from seawater. Very particular combinations of materials would be required to produce a large ice cake that could be entrained deep into the water column. Mechanisms for the production of large ice cakes fundamentally depend upon buoyant force, a large tidal range, and hypsometry having deep channels cut through tidal flats. We document the unlikely set of events that would be required in order to produce large ice cakes that are sufficiently near neutral buoyancy and also drift into the Minas Passage so as to pose a danger to large in-stream tidal turbines.

* Corresponding author.
E-mail addresses: bxs@eastlink.ca (B.G. Sanderson), Anna.Redden@acadiau.ca (A.M. Redden).

http://dx.doi.org/10.1016/j.ijome.2015.01.006
2214-1669/

1. Introduction

Increasingly it is becoming clear that global reliance upon fossil fuels has adverse consequences [1] and is not sustainable in the long term [2]. Renewable energy resources, including tidal energy, are currently being developed. Technologies for using tidal energy have a long history and now include tidal in-stream energy conversion (TISEC) devices. There is interest in large-scale extraction of tidal energy from many sites around the globe [3]. Many prominant sites (including Ungava Bay and the Bay of Fundy in Canada) have large tidal ranges and are also at high latitude where ice forms.

Strong (up to ~5 m/s) semidiurnal tidal currents make Minas Passage (Bay of Fundy) a site from which a large amount of electrical power might be obtained [4] given cost-effective deployment of durable TISECs. TISEC survivability remains to be demonstrated at this dynamic site [5]. Beyond the obvious difficulties posed by strong currents, Sanders [6] expresses a view that large sediment-laden ice cakes might be found at depth within the water column and contends that *'the major engineering issue presently facing the harvest of tidal electricity from the upper Bay of Fundy is the danger that non-buoyant ice and other subsurface masses may pose to submerged tidal current harvesting devices'*.

Minas Basin has tidal ranges up to 17 m that are the highest on Earth. During winter, large quantities of ice form on tidal flats and where rivers run into Minas Basin [7]. Large ice cakes are generated in the intertidal zone in Minas Basin and are commonly observed in the Cobequid Bay and Avon/Cornwallis River regions (Fig. 1).

Ice rafting of sedimentary material has been long recognized [8]. Hind [9] published the first observations of sediment-laden ice floating in the Bay of Fundy and the matter has been elaborated upon in more recent works [7,10]. This raises a possibility of large sediment laden ice cakes that are near

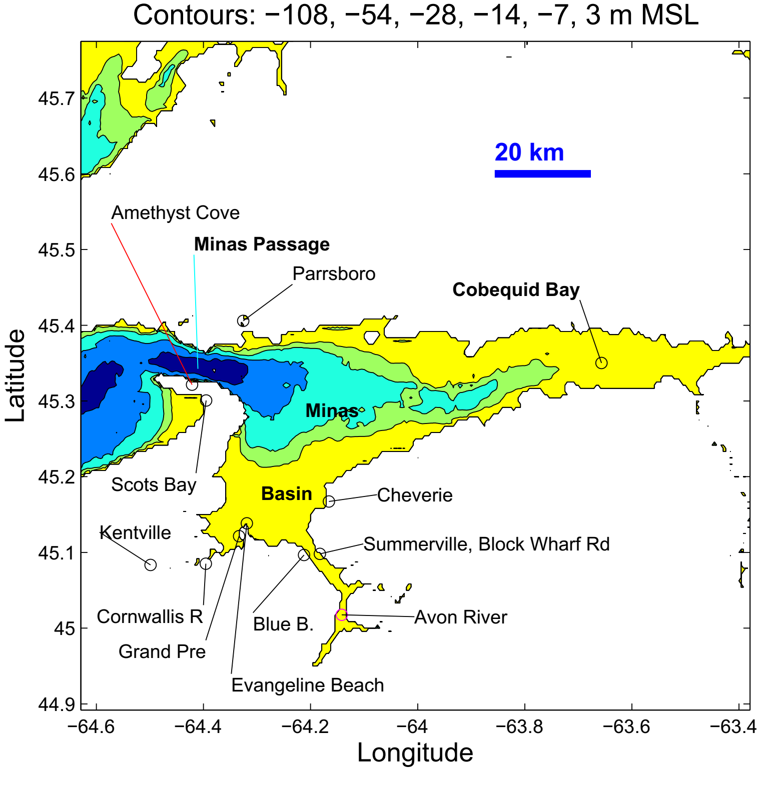

Fig. 1. Bathymetry of Minas Basin and Minas Passage, ~500 m horizontal resolution. Labelling indicates sites and place names referred to in the text.

neutral buoyancy. Considering bathymetry and the range of spring tides, about 60% of the volume of Minas Basin flows in and out through Minas Passage with each spring tidal cycle. Spatio-temporal variation of strong tidal currents generally causes substantial stirring due to the Lagrangian chaos mechanism [11] so neutrally-buoyant ice cakes—if they exist—are expected to commonly mix onto water-mass trajectories that reach Minas Passage. There is a *prima facie* case that sediment-laden ice cakes might be advected into Minas Passage where they might affect the survivability of TISECs. The following work will investigate the danger that ice cakes might pose to TISECs. Risk of this danger most fundamentally hinges upon the abundance of large neutrally-buoyant ice cakes.

2. Observations, results and analyses

2.1. Summary of methods

The danger that sediment laden ice might pose to TISECs is a function of many mechanisms and requires a multifaceted understanding of ice cakes. Throughout our analysis we integrate observations, measurements and mechanical theory. A thematic development is required: starting with formation, movement and transformation of large sediment-laden ice cakes; progressing to sampling and measurement of ice cakes with characteristics deemed likely to make them a threat to TISECs; thence considering how tidal turbulence influences the vertical displacement of ice cakes of different sizes and densities. Having examined these prerequisites, we identify the suite of events necessary in order for large ice cakes to collide with a TISEC deployed in Minas Passage. Finally we consider a scaling of the size of TISECs in view of the forces imposed by currents and ice cakes.

Use will be made of many types of measurements and observations, made at a variety of sites. Locations are shown in Fig. 1. Measurements and observations will be introduced in the sequence with which they are utilized.

2.2. Production of large sediment-laden ice cakes

Waters in Minas Passage have salinities in the range 31–32 ppt [12,13] and flow in and out of Minas Basin over the tidal cycle. Upon cooling, seawater with salinity more than 24.7 ppt will reach its temperature of maximum density before freezing [14]. Through most of Minas Basin, salinity and vertical mixing are sufficiently high so the entire water column must cool to freezing before offshore ice formation occurs. Nevertheless ice does sometimes form offshore in Minas Basin and it is famously reported [15] that Ebenezer Bishop used a notched board to "walk" across the ice-jammed Minas Passage from Amethyst Cove to Parrsboro (Fig. 1) on 14 February 1809. On the basis of more recent observations, every three to five years there will be periods with ~30% cover of ~0.15 m thick ice in floes with ~100 m length scale [6]. It is noteworthy that water depth increases greatly going from Minas Basin into Minas Passage. Thus, on the outflowing tide the water column is stretched and surface convergence will concentrate ice floating into Minas Passage, explaining the abovementioned ice-jamming. Surface ice is not expected to collide with a TISEC that is well beneath the surface.

In northern temperate estuaries during winter, bottom sediment can become frozen within the intertidal zone where sediment is exposed for sufficiently long periods while the tide is low. Subsequently, both sediment-water and atmosphere-water heat fluxes contribute to formation of frazil ice as the tide rises over a broad intertidal zone. Frazil ice was observed in the shallow waters adjacent Evangeline Beach on 16 February 2011 when the salinity was 29.3 ppt. The Kentville, Nova Scotia meteorological station recorded an average air temperature of −9.3 °C for that day, reducing water temperature to −1.5 °C. A strong onshore wind resulted in a 0.06 m layer of frazil ice being deposited on Evangeline Beach when the tide had receded (Fig. 2). The 30-year average air temperatures at Kentville weather station—December −0.7 °C, January −4.1 °C, February −2.7 °C, and March −0.1 °C—indicate such freezing is not unusual for the months of January and February.

Such frazil ice formation and freezing of freshwater discharged from the catchment, are the genesis of ice cakes. Frazil ice can mix with uncompacted sediment [16], freeze onto sediment and acumulate onto existing ice cakes. Suspended sediment concentrations can be high [17] resulting in the

Fig. 2. Ice cake 1 at Evangeline Beach (45.13834° N, 64.31901° W) on 16 February 2011. The photograph shows the remaining portion of the ice cake after sectioning and removing samples for density measurement. Total length of the axe is 0.835 m. Frazil ice has been deposited on the beach with the falling tide.

deposition of coarse silt upon ice. Direct snowfall and other freezing precipitation, adds to the mass of ice, particularly for ice cakes stranded high in the intertidal zone. Wind, waves and tidal currents can cause pieces of ice to raft one on top of the other, or to otherwise aggregate, forming larger ice cakes with subsequent freezing. Sectioned ice cakes typically exhibit complex patterns of layering, aggregation and stacking (Figs. 2 and 8).

Large ice cakes are formed in the nearshore and are frequently observed stranded on tidal flats [18]. This is to be expected, given that the nearshore hypsometry is typified by narrow, deep tidal channels running through extensive areas of tidal flats. The water column is vertically compressed (horizontal divergence) as water flows from deep channels to cover shallow flats. A piece of floating ice has a fixed draft so the flood tide can only advect it shoreward to the point where it becomes grounded, to be left stranded upon the falling tide—or until its shoreward motion is blocked by the abundance of ice that has previously been transported onto the tidal flat. The top photograph in Fig. 3 shows ice cakes packed onto a beach on 18 February 2011.

Fields of stranded ice can be rapidly transported offshore when a high tide floats buoyant ice cakes and strong winds blow them offshore (bottom photograph of Fig. 3). The transition illustrated by Fig. 3 resulted from spring tides and strong northerly winds observed during the 20 February high tide.

Without wind, there are still mechanisms that result in some previously stranded ice being moved offshore with the falling tide. Consider, for example, an ice cake that has become frozen to the bottom (or trapped amidst other land-fast ice) but is broken free by buoyancy forces after becoming totally submerged by the high tide. Near high tide, an aware observer will frequently see (and hear) a buoyant ice cake bob to the surface after breaking free from the frozen bottom. The floating ice cake can then be transported offshore by the falling tide.

Stranded ice cakes may freeze tightly to bottom substrate. On the rising tide, a sufficiently buoyant ice cake may tear up a portion of the bottom which remains incorporated as part of the floating ice cake. This mechanism has been dubbed 'plucking' by Black [16]. Critical for our purposes, it is important to point out that after the plucking event the resulting ice cake must be buoyant. Sometimes such plucked material may be rafted some distance before becoming detached. For examples of such detached material, on 23 and 25 February 2011 we observed isolated clumps of saltmarsh sediment containing *Spartina* at Cheverie (45.16736° N, 64.16587° W) and Summerville (45.09792° N,

Fig. 3. Views from Block Wharf Rd, Summerville (45.09813° N, 64.18271° W). Top: Stranded ice covers the beach on 18 February 2011. Bottom: Tide and wind have removed most ice from the beach by 22 February 2011.

64.18286° W) which had been transported at least 1 km, based on the location of the nearest saltmarsh habitat.

Vertical ice walls form at the edges of channels in the upper reaches of the Bay of Fundy [10]. The base of these vertical ice walls begins a little below the level of the lowest tides during the period in which the ice wall was formed [10,16]. Black [16] measured a sequence of channel cross sections from the time of ice wall formation until disintegration of the ice wall, and has used time-lapse photography to create a video that illustrates transport of ice within a tidal channel and adjacent flat (Black, pers. com.). To augment this previous work, we will next demonstrate that a fundamental mechanism of ice wall formation follows from our previous description of tidal transport of buoyant ice cakes into shallow water.

A staggered leap-frog discretization with wetting and drying is used to model a barotropic tide as it rises and falls over bathymetry consisting of a steeply sloping side of a channel that gives way to a slightly sloping saltmarsh (Fig. 4). A floating ice cake moves shoreward with the water on the rising tide. The ice cake floats with a constant bottom clearance so long as the water level remains below

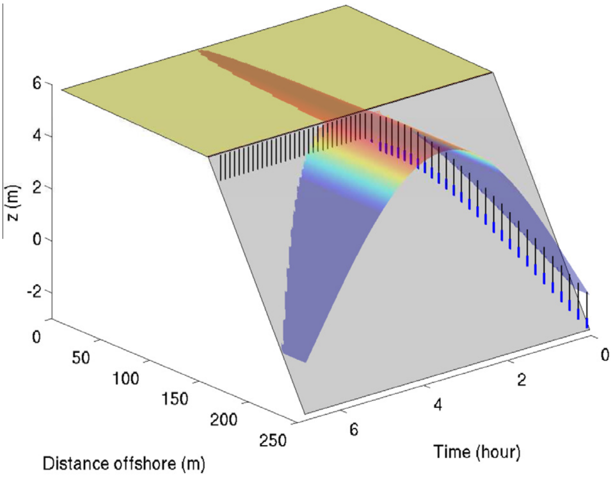

Fig. 4. Water level of the tide is shown as a function of time and distance offshore (multi-colored surface). The rising tide carries an ice cake (vertical black line) up the side of a steep channel. At first there is bottom clearance (blue) beneath the ice cake. The ice cake becomes stranded when the tide flushes over the gently sloping salt marsh (green surface). (For interpretation of the references to colour in this figure legend, the reader is referred to the web version of this article.)

the level of the saltmarsh (Fig. 4). A column of water advecting with the flow is merely translated upwards and shorewards as the tide rises up the steep, uniformly sloping side of the channel. The situation is quite different when the tide rises further and floods the slightly sloping saltmarsh. At that time, a column of water moving with the flow becomes vertically compressed (divergence of the current) whereas the ice cake has a fixed draft and so it becomes grounded within the upper part of the channel (Fig. 4). When the tide retreats, grounded ice can freeze to: the bottom, adjacent ice, stranded frazil ice, freezing precipitation, and freezing water that drains from the saltmarsh after the tide has fallen. Once such ice is frozen in place, it becomes a new surface with nooks and crannies, upon which and within which floating ice can be trapped as it is transported by the next tide. Subsequent tides will result in further trapping and the freezing in place of ice cakes until a vertical wall is formed that extends into water that is too deep to trap further ice cakes, at which point the mechanism for further trapping fails. Ice walls in the Bay of Fundy can have a vertical extent of 5 m [10].

Black [16] suggests that the largest ice cakes form when ice walls slump from the edges of narrow channels. Such slumping might be a result of undermining by meltwater (or other warm water) draining from the adjacent flats, augmented by warmed estuarine water that erodes the base of the ice wall [7]. Warming of the nearshore estuarine water can be substantial under sunny conditions, presumably due to the low albedo of sediment. This is demonstrated by measurements made early on the rising tide, 1100 on 8 March 2011 at Summerville, when nearshore water had been heated to 2.2 °C whereas it was only 0.7 °C a little offshore in water ≈1 m deep. (Air temperature was −1 °C.) Measurements at 1320 h continued to show that water temperature increased progressing shoreward into shallowing water; temperatures of (0.5, 1.5, 2.4) °C corresponding to locations where water depths were (1, 0.5, 0.1) m, respectively.

Given the above mechanisms, the size of the largest ice cakes is intrinsically tied to the tidal range because tidal range determines the depth of tidal channels cutting through sediment flats in the upper reaches of Minas Basin. Additionally, the height to which the ice wall can be built is limited by the tidal range required to float additional ice onto the crest of the existing ice wall.

2.3. Density measurements

The fundamental question is how common are near neutrally-buoyant ice cakes within the Minas Passage, where TISECs are to be deployed. Density of ice might be calculated according to its salinity and temperature [19] providing there are no air pockets or sediment within the ice. Measurements of salinity, sediment content, and air pockets do not afford a practical determination of ice density. What is required are direct measurements of the *in-situ* density of ice as it naturally occurs. Given rafting of frozen sediment, it is also relevant to measure the density of frozen sediment.

Two sediment samples were obtained from near the seaward edge of the saltmarsh at Grand Pre (45.1117° N, 64.0391° W) on 4 December 2010. Sediment was mostly firm, compacted, cohesive material overlain by a thin (0.01–0.02 m) reddish layer that was soft and readily resuspended by small waves. The sediment samples were placed directly into containers, sealed and frozen in a freezer. Densities of the frozen samples were measured using Archimedes Principle. The sediment sample from the lower, unvegetated site had density $1800 \pm 25\ \mathrm{kg/m^3}$ (± indicates measurement error) whereas the sample from the more elevated, vegetated site had density $1660 \pm 20\ \mathrm{kg/m^3}$. Sediment is expected to vary somewhat from site to site but the important point is that frozen bottom sediment is substantially more dense than seawater—to a similar extent that air pockets are less dense.

Ice cakes are usually too massive to manually manipulate and directly measure using inexpensive, portable tools. Using a hand saw with carbide teeth, ice cakes were sectioned vertically in the field and divided into layers (numbered from top to bottom), with three to five ice samples taken from each layer. Ice samples had a typical size of about $0.3 \times 0.3 \times 0.2\ \mathrm{m^3}$. The density of each sample was immediately measured in the field by immersion in a container of local seawater and application of Archimedes Principle, as follows.

Salinity and temperature of the seawater were measured so that the seawater density ρ_{sw} could be calculated using the UNESCO equation of state [20]. The practical-mass of a floating ice sample can be determined from the volume V_f of water that it displaces while freely floating. Thus the practical-mass is $\rho_{sw}V_f$. Define the practical-volume of an ice sample as the volume of seawater V_s that it displaces when it is fully submerged within a container of seawater for a short time. Thus, the practical-density (henceforth density) of a buoyant ice sample is

$$\rho = \rho_{sw}\frac{V_f}{V_s} \tag{1}$$

In the instances when the ice sample sank, the ice sample was placed on top of styrofoam so the joint styrofoam-ice volume and density could be measured as above and the ice density backed out from the known mass and volume of the styrofoam.

The geometry of an ice cake is not simple to quantify. Ice cakes have air cavities of various sizes so there is no clear separation into a macroscopic surface that encloses an ice cake volume and smaller scale cavities that can be separately considered as porous spaces. Practical-porosity (henceforth porosity) was estimated by considering the volume of water V_r removed from the container when the submerged ice cake is lifted from the container in a smooth, deliberate, consistent motion. Thus, the porosity was calculated using

$$\text{Porosity} = \frac{V_r}{V_s + V_r}. \tag{2}$$

Porosity was only measured if the ice sample floated. Porosity measurements are expected to be relevant to TISEC-ice collisions because porosity may be related to: strength, melting, and topology of partially melted ice cakes. Strength and melting were not measured in the present study.

In February and March 2011, ice cakes were sectioned and measured at locations (Fig. 1) as follows: Evangeline Beach (45.13834° N, 64.31901° W), Blue Beach (45.09667° N, 64.21221° W), Summerville near Block Wharf Rd (45.09813° N, 64.18271° W), and Grand Pre near West Long Island Rd (45.12154° N, 64.33353° W). In all, 123 ice samples were cut from 8 large ice cakes and an ice wall. No pretense can be made that this is a statistically representative sampling of all the ice cakes in Minas Basin. Fig. 3 illustrates that the vast majority of ice cakes must be buoyant, as discussed previously. Our objective was to explore the existence of ice cakes that might be nearly neutrally buoyant, so our measurements are biased towards sampling ice cakes that had significant sediment load.

Sanders [6] suggests that heavily stained ice cakes may be sufficiently dense in order to be near neutrally buoyant and claims that: *"Cakes whose gross appearance suggests they may exceed this sediment composition are easy to find in the Upper Bay."* Black [16] has hypothesized that melting might concentrate the sediment, leaving a more dense ice cake. Fig. 5 shows an ice cake that has the

Fig. 5. Ice cake 6 at Grand Pre, West Long Island Rd, on 7 March 2011. GPS 45.12154° N, 64.33353° W. Total length of the axe is 0.835 m and the hand saw is 0.80 m long.

appearance of being more heavily stained than the example shown by Sanders [6]. We measured this heavily stained ice cake on 7 March 2011 prior to which time ice melt had been observed, presumably increasing sediment concentration. Densities of samples cut from this ice cake were in the range 830–870 kg/m^3, all very buoyant. Fig. 6 shows another sediment stained ice cake that is being melted by solar radiation on 23 February 2011. Melted water drains free from the sediment at which stage it absorbs less radiation and quickly becomes frozen because of sub-zero air temperatures. A soft, muddy deposit is left behind and this was observed to wash away when immersed in seawater. Contrary to previous expectations [6,16], melting does not necessarily increase the sediment concentration of a sediment stained ice cake and heavy sediment staining does not indicate high density.

All samples that had density greater than that of seawater also contained coherent portions of bottom material (rocks, gravel or frozen bottom sediment) that had been incorporated by ‘plucking’. It is notable that the density of ice is substantially less than the density of seawater in Minas Passage whereas the density of frozen bottom sediment is very much higher. Similarly, samples cut from within ice cakes tend to be either much more dense or much less dense than the seawater in Minas Passage (Fig. 7). We preferentially sampled ice cakes that exhibited ‘plucking’ so Fig. 7 almost certainly over represents high density samples relative to what might be obtained by randomly sampling the total population of ice cakes. The important point is that one has to go to some trouble to select an ice cake and then cut a neutrally buoyant sample from it. Clearly, random sampling of the entire ice cake population would make it even more difficult to cut out a neutrally buoyant sample and would confound our objective: *viz.* to explore the existence of neutrally buoyant ice cakes.

Finding an ice cake that is not buoyant seems near impossible within a field of ice cakes like that shown in the top photograph of Fig. 3. Once a tide-wind event clears the area of many of the buoyant ice cakes, it might become more feasible to find an ice cake with neutral or negative buoyancy.

Ice cake 4 was first observed at Summerville on 22 February 2011 (Fig. 8) after the wind-tide event had cleared most of the buoyant ice cakes from the beach. Layer 1 (top) of ice cake 4 became completely detached during sampling, leaving a base which was sampled as layers 2 and 3. Samples taken from ice cake 4 (Table 1) indicated that what remained after sampling (the base) might be nearly neutrally buoyant and probably tended towards being negatively buoyant. The ice cake was observed as the tide rose over it. It appeared, briefly, to move with the fast-flowing tide although the water was highly turbid and turbulent so it was difficult to be certain. GPS coordinates were obtained for ice cake 4 at subsequent low tides and positions are plotted in Fig. 9. Ice cake 4 moved a short distance (≈20 m) during the period 22 to 23 of February. The direction of motion was up-estuary and down the beach slope so this movement is consistent with our brief (and tentative) observation.

On 25 February 2011, ice cake 4 was melting (Fig. 8) and by 8 March it was entirely gone. Radiative heating is mostly responsible for the melting, which is far greater on the side exposed to the sun. Any ice cakes that might have made it as far as Minas Passage would be exposed to relatively warm water compared to the then subzero temperature of the Avon River, given measurements at Scots Bay (Fig. 1) gave salinity 32 ppt and water temperature of 2.5 °C at 1344 h on 25 February 2011.

Fig. 6. Ice cake 5 at Summerville, Block Wharf Rd, on 23 February 2011. The sunny side of a sediment-stained ice cake is melted by solar radiation. Average air temperature was −6.4 °C at Kentville. Meltwater separates from sediment and refreezes. Note the complex geometry of layers and air pockets.

Fig. 10 shows that there is a clear trend for porosity to be higher nearer the tops of the ice cakes. Different ice cakes had different vertical dimensions, so the number of layers was variable. Negatively buoyant samples were almost always found near the bottoms of ice cakes where porosity is low. When an ice cake melts by contact with warmer water, the most porous material will have the highest ratio of contact area to volume and may be subject to the greatest rate of melt, in which case one might expect overall density of the ice cake to increase. This hypothesis has not been tested, although it might be testable by observing the progressive melting of ice cakes as they are carried by the currents offshore. In lieu of such observations, Fig. 11 shows a photograph of an ice cake floating nearshore at a time (1044 h on 8 March 2011) when light winds blew onshore and up estuary. The ice has a skeletal topology and seems to have undergone substantial melting. Notably, sediment seems to have been washed out, leaving a skeleton of clear ice. This skeletal ice cake obviously has less ice mass and less strength than would solid ice with the same overall dimensions. Given the large amount of surface area for a relatively small mass of ice, it is conceivable (but has not been observed) that such skeletal properties make an ice cake more prone to being dragged to depth should it ever migrate into the roiling currents in Minas Passage—even though the skeletal ice cake is clearly buoyant.

2.4. Vertical motion of ice

Breaking wind-waves sometimes push small particles of buoyant ice downwards into the water column. Strongly flowing tide causes turbulent vertical motion. Vertical currents can drag a particle downwards even if that particle has density different from the water in which it is immersed.

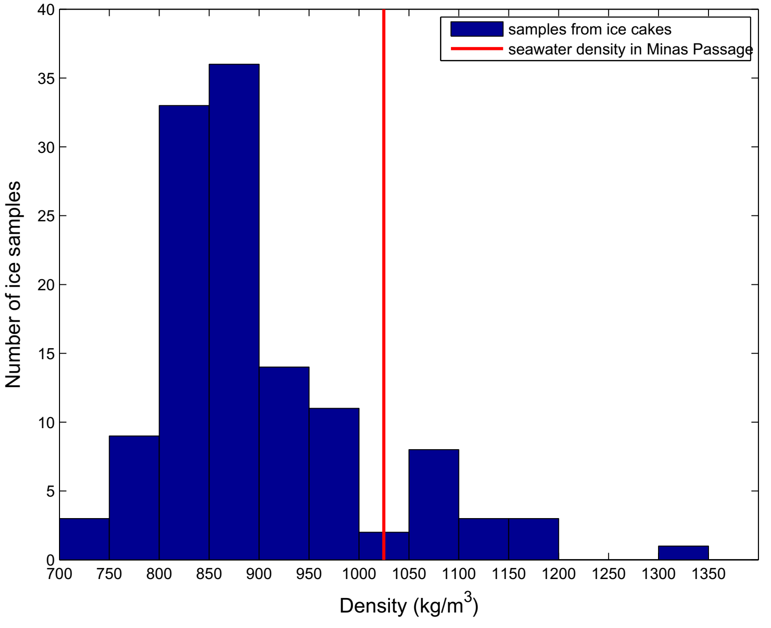

Fig. 7. Histogram of density of samples from ice cakes, including samples from the ridge ice.

Consider the vertical current speed to be w. Denote the cross-sectional area of an ice cake as A_i, its volume as V, and density ρ. The magnitude of the drag force scales as $(1/2)C_d\rho_{sw}A_iw^2$ where C_d is a drag coefficient. The magnitude of the buoyancy force scales as $g|\rho_{sw} - \rho|V$. Thus, there will be a critical vertical current w_c at which these forces balance. Equating drag to buoyancy enables calculation of the vertical current w_c that might drag a particle into the interior of the water column.

$$w_c = \sqrt{\frac{2\,g|\rho_{sw} - \rho|V}{C_d\rho_{sw}A_i}} \tag{3}$$

Eq. (3) applies in both the upwards and downwards sense, depending upon whether a particle is more dense or less dense than the water in which it is immersed.

Presently, the key idea is that w_c is proportional to $\sqrt{\ell}$ where $\ell = V/A_i$ is a characteristic length scale for the ice cake. All else being equal, small pieces of ice are relatively easy to entrain into the water column compared to large pieces of ice. Hay (pers. com.) measured horizontal and vertical components of current in Grand Passage (Bay of Fundy) and found that the standard deviation of turbulent vertical motion was 1.2 times the friction velocity and the (quadratic) bottom drag coefficient was 12×10^{-3} with a reference level of 1 m above the bottom. Based upon these results, it is reasonable to set a scale for w_c that is about one-tenth the horizontal component of tidal current. Proportionate scaling of turbulent speed and larger scale current is broadly consistent with theory for turbulent boundary-layer flows [21].

In Minas Passage the tidal currents can be as high as 5 m/s so we will take 0.5 m/s as a scale for w_c. It is then possible to use (3) to calculate the upper limit for the density difference $|\rho_{sw} - \rho|$ that an ice cake can have and still be dragged into the interior of the water column. Table 2 shows that this density difference can be quite large for a small ice cake but becomes very small for a larger ice cake. The likelihood that large ice cakes will be entrained into the interior of the water column is very low compared to the likelihood for entrainment of small pieces of ice.

Typical densities of ice samples (Fig. 7) are about 150 kg/m^3 less than the density of seawater so it is relatively likely that 1 kg pieces of ice, $\ell \sim 0.1$ m, might impact a TISEC deployed in Minas Passage.

Fig. 8. Top: Ice cake 4 at Summerville, Block Wharf Rd, on 22 February 2011. GPS: 45.09811° N, 64.18322° W. The total length of the axe is 0.835 m. Ice cake 4 was melting in the sunshine on 25 February 2011. Middle: The side most exposed to the sun. Note sediment washed off the melting ice cake. Bottom: The side least exposed to the sun.

On the other hand, a 1 tonne ice cake, $\ell \sim 1$ m, would need to match the density of seawater to within 13 kg/m^3 for it to be dragged to depth. It seems relatively unlikely that an ice cake, composed mostly of material that is typically 150 kg/m^3 less dense than seawater (Fig. 7), would be ballasted with just the right amount of sedimentary material in order to bring its density within 13 kg/m^3 of the density of seawater.

2.5. Likelihood of collision

Collision of a dangerously-large ice cake ($\ell_{\text{dangerous}}$) with a TISEC depends upon an irreducible set of events and conditions:

Table 1
Density and porosity of ice cake 4 at Summerville, Block Wharf Rd (45.09811° N, 64.18322° W) on 22 February 2011.

Ice cake 4	Density (kg/m^3)	Porosity
Layer 1	789	0.0638
	801	0.1096
	817	0.0678
	832	0.0000
Layer 2, top of the base	873	0.0159
	856	0.0312
	823	0.0270
	823	0.0270
	891	0.0351
Layer 3, bottom of the base	1172*	
	1112*	
	1062*	
	1169*	
	1073*	
	1060*	
Vertical section of the base	964	
	992	
	983	
	941	0.0377
	917	0.0167
	1074*	
	1174*	

* Indicates densities greater than those of the local seawater (1021.1 kg/m^3).

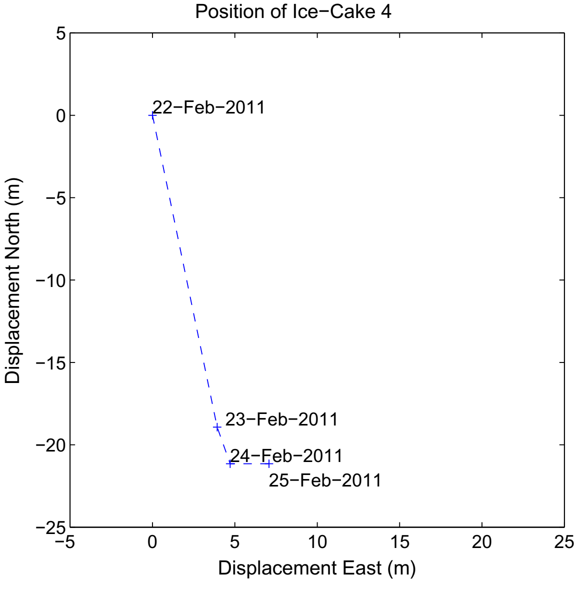

Fig. 9. Positions of the negatively buoyant ice cake 4. To within the accuracy of measurements, position does not change after 23 February 2011.

1. A still larger buoyant ice cake ($\ell^3 \gg \ell^3_{\text{dangerous}}$) must form and become grounded in the intertidal zone. (Many ice cakes do become grounded.)
2. It must strongly adhere to dense, frozen sedimentary material.

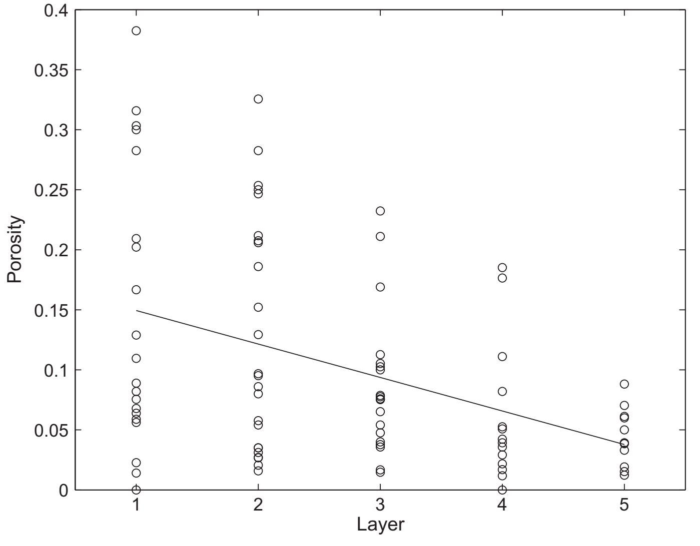

Fig. 10. Porosity of ice samples plotted against the layer number from which they were cut. The top layer is number 1. The line shows a best fit linear regression: Porosity = 0.18 – 0.28 × Layer ($R^2 = 0.2$). *Note*: porosity was not measured for negatively buoyant samples.

Fig. 11. The clear skeletal remains of an ice cake, Summerville, Block Wharf Rd, 8 March 2011. A small coherent block of sediment-stained ice is perched on top.

3. It must have sufficient buoyancy to tear off a portion of the frozen sediment when tide is high. Thus, the resulting ice cake (including the recently attached sediment) must have an overall positive buoyancy.
4. The buoyant ice cake must differentially melt or fracture, so less dense ice is lost preferentially to dense sedimentary material. Antithetically, there are observations of rafted material deposited in the intertidal zone which demonstrates that the more dense material is lost, making the ice cake

Table 2
An upper limit on density difference $|\rho_{sw} - \rho|$ that permits an ice cake with length scale ℓ to be dragged into mid water-column by turbulence resulting from 5 m/s tidal currents. The drag coefficient was $C_d \approx 1$.

ℓ (m)	Nominal ice-cake mass (kg)	$\|\rho_{sw} - \rho\|$ (kg/m^3)
0.1	1	130
0.5	130	26
1.0	1000	13
1.5	3500	8.7
2.0	8200	6.5
2.5	16,000	5.2
3.0	28,000	4.3

more buoyant. Internal stresses within an ice cake might be expected to be increased at discontinuities, such as where dense material attaches to the buoyant ice. Our observations also indicate that melting can cause preferential loss of dense sedimentary material.

5. Any remaining ice cake must be sufficiently large and sufficiently strong to be a danger.
6. The remaining ice cake must have a density that falls within a narrow range in order that turbulence can move it vertically through the water column—the larger the ice cake, the smaller the density range. Collisions with large ice cakes are, therefore, less likely than collisions with small ice cakes.
7. Currents must have transported the ice cake to Minas Passage where TISECs are deployed.
8. Size and density must persist for a sufficiently long time to cause a significant collision cross-section with a TISEC in Minas Passage. This is made less likely because water warms going westward through the Minas Passage.

With respect to steps 7 and 8, Smith et al. [22] fixed GPS-equipped satellite transmitters to 9 buoyant ice cakes at various nearshore sites within Minas Basin in March 2009. Trajectories of some of the transmitters were clearly influenced by grounding. Three of the transmitters reached Minas Passage and were retrieved (free from ice) west of Scots Bay. Another transmitter, deployed at Lower Truro (at the head of Cobequid Bay), at first went upriver but subsequently tracked into open water and travelled across Minas Basin. Such large-scale mixing—from rivers to the open waters of Minas Basin and beyond—is expected given the mixing of oscillating flows in a multi-channel system [23] and Lagrangian chaos in general [11].

The danger of subsurface ice to TISECs is a multiplicative process, equal to the number of ice cakes in step 1 multiplied by the product of probabilities of processes in steps 2 through 8. This joint probability problem is akin to the "Drake Equation" [24] and is similarly confounded by poorly known constituent probabilities and the lack of a single observation of the sought-after entity.

Evaluating the probability that some randomly selected ice cake is sufficiently near to neutral buoyancy is beyond the realm of present observations—except to say that our observations and results are consistent with a very low likelihood. However, we can propose a way forward, based upon the mechanism that leads to vast numbers of ice cakes becoming stranded in the upper intertidal zone at low tide. Floating ice cakes are transported over rising bathymetry with the rising tide, so they become stranded after being grounded near high tide. A neutrally buoyant ice cake can be anywhere within the water column, so it is not constrained to move with the surface waters and is expected to have a higher probability of being stranded low in the intertidal zone at low tide. If we look offshore at low tide and see 1000 ice cakes grounded high in the intertidal zone and 10 ice cakes grounded low in the intertidal zone then it is reasonable to conclude that the probability of ice cakes being of near-neutral buoyancy is less than 0.01. Further, it would seem to be relatively easy to refine the probability if we were to observe which of the 10 lower ice cakes floated upon the rising tide.

2.6. Scaling turbines and ice cakes with respect to tide

Having seen that the relative likelihood of ice–TISEC collision scales according to the size of ice cakes and current speed, we now explore the scaling of forces between ice cakes and a TISEC installation relative to other forces that affect the installation. More sophisticated modeling of forces and deformations due to impact [25] is beyond the scope of the present scaling analysis and would require much more knowledge of both the mechanical properties of ice and structural details of a specific installation.

Consider the force applied by a neutrally buoyant ice cake (density $\rho = \rho_{sw}$) of dimension ℓ when it impacts a turbine installation. The ice cake has the same mass $M = \rho_{sw}\ell^3$ and momentum $\rho_{sw}\ell^3 U$ as the water that it displaces but the ice cake is not so deformable as water. Let the ice cake squarely strike an installation making contact over an area A_c. Model the collision as a two stage process. First we expect deformation of the installation as though it had spring constant k. Second, there will be deformation (possibly fracture) of the ice cake if the contact force reaches the strength of the ice cake. Compressive strength and flexural strength have been measured for large-scale sea ice in the arctic [26,27] but not for the ice cakes found in the Bay of Fundy—although it is easy to section and fracture ice cakes using simple tools: a hand saw and an axe. Denote the compressive strength of ice cakes as S.

In the first (elastic) stage of the collision, kinetic energy of the ice cake $\frac{1}{2}MU^2$ deflects the structure by a distance

$$D = \min\left(\sqrt{\frac{M}{k}}U, \frac{SA_c}{k}\right) \tag{4}$$

as kinetic energy is transferred into potential energy of a spring. If $\sqrt{Mk}U \leqslant SA_c$ then the ice cake applies a peak impact force

$$F_{\mathrm{impact}} = kD = \sqrt{Mk}U \tag{5}$$

to the structure and the second stage does not apply.

If $\sqrt{Mk}U > SA_c$ then at the end of the first stage the ice cake will have kinetic energy

$$\frac{1}{2}MU_2^2 = \frac{1}{2}MU^2 - \frac{1}{2k}(SA_c)^2 \tag{6}$$

Thus, during the second stage the ice cake applies an impulse

$$I = \sqrt{M^2U^2 - \frac{M}{k}(SA_c)^2} \tag{7}$$

and the force of the ice cake impact is SA_c with duration $\delta t = I/(SA_c)$.

Note, the above calculation is nonspecific as to which part of the TISEC is impacted. For some designs, and for some purposes, it may be desirable to calculate impact forces upon the blade tip. The above equations would still apply but with U being the water velocity relative to the blade tip.

Turbine installations in Minas Passage could use gravity based stability [5]. Drag forces of water upon the turbine installation scale as

$$F_{\mathrm{drag}} \sim L^2U^2 \tag{8}$$

where L is a characteristic length scale for the installation. Similarly, the power-producing lift force F_{lift} also scales as L^2U^2 but with a different proportionallity constant from that for drag. Gravitational forces depend upon equipment mass and therefore scale as L^3. It is necessary for $F_{\mathrm{grav}} > F_{\mathrm{drag}}$ in order for gravity to stabilize the installation against drag so the following scaling relationship is required

$$L \sim U^2 \tag{9}$$

This shows how a gravity-based turbine installation that has been designed and tested to work at lower current speeds should be scaled in order to work in a high current site, like Minas Passage.

Given (9) it follows that the mass of a turbine installation should be scaled as L^3 or U^6. Power P output from the turbine scales as the rate at which work is done by the lift force

$$P \sim F_{\mathrm{lift}}U \sim L^2U^2U \sim U^7 \tag{10}$$

Strength of the turbine installation scales as L^2 (equivalently U^4) whereas the drag forces that the turbine must withstand will scale as U^2.

On 12 November 2009 a 1 MW TISEC that was deployed in Minas Passage failed on 4 December 2009 when current speed was more than twice what had been expected [5]. Assuming that a TISEC is reliable in 2.5 m/s currents, it is worth considering how the machine might be modified to operate in 5 m/s currents. The length scale would be increased by a factor of 4, strength by a factor of 16, mass by a factor of 64 and power output by a factor of 128. Thus, neglecting ice cake collisions, a gravity-based turbine installation should have improved survivability and be more cost-effective when appropriately scaled for higher current locations.

Consider ice cake collisions having impact forces that scale according to (5) where stiffness k scales proportional to L. Considering ice cake mass M to be invariant, then a doubling of U would correspond to ice impact forces being increased by a factor of 4 which is small relative to the corresponding factor of 16 increase in the strength of the installation scaled for U. On the other hand, if we consider the length scale of ice cakes to scale with tidal range, and tidal range to scale with U, then a doubling of U would correspond to the ice-cake mass M being increased by a factor of 8 and impact force being increased by a factor of 32 which is more than the corresponding factor of 16 increase in the strength of the installation. This latter scaling illustrates that the possibility of dangerous collision with a subsurface ice cake is most fundamentally tied to the expectation that ice cake mass is related to tidal range. Ultimately, the situation is not so severe as obtained by the latter scaling because at sufficiently large scales the ice cake strength S limits impact force to SA_c rather than (5). Regardless, a larger scale machine is more robust for a given environment.

3. Discussion

Sediment stained ice cakes in the upper Bay of Fundy demonstrably float and are not a danger to TISECs. Most samples cut from ice cakes are very buoyant. Samples that are not buoyant were observed to contain coherent portions of frozen bottom substrate, consistent with benthic material being incorporated into the necessarily buoyant ice cake via the 'plucking' mechanism. Observations show that such plucked material is sometimes dropped, harmlessly to the bottom, leaving the ice cake even more buoyant. Similarly, differential melting can sometimes cause ice cakes to become more buoyant.

On the other hand melting had a quite different effect upon an ice cake that was artificially fractured to create a flat lower portion that was negatively buoyant but was still able to be moved a short distance by the strong tides. Subsequently, solar radiation melted the top surface of the stranded ice cake which rendered it immobile when inundated by strong tidal currents.

Physical scaling arguments show that in order for an ice cake to be swept deep into the water column, the density of the ice cake must be within a narrow range that scales inversely with its length scale. Constituent materials within ice cakes (ice, air pockets, salt, sediment) have densities that are quite different from that of seawater, so a large ice cake requires particularly unusual combination of such materials in order to be within such a narrow density range. Thus, the probability of a TISEC being hit by a large sediment-laden ice cake is far lower that the probability of it being hit by a small piece of ice.

Without consideration of ice, dynamical scaling of gravity-based in-stream turbine installations suggests that the scale of the turbine L should be increased proportional to the square of current speed U^2. Such scaling indicates that machine survivability and power output would be favorably enhanced in high-flow areas, like Minas Passage.

Consideration of mechanisms producing ice cakes indicates that the size of ice cakes should increase as tidal range increases. Also, stronger tidal currents can entrain bigger ice cakes to depth within the water column. This suggests that the size of TISECs should be scaled according to tidal range and current in order to ensure that turbines are robust to collision with any subsurface ice. Compressive and fracture strength of ice cakes are expected to be important for such scaling but these are unknown. For this reason, it remains unclear how the scale of TISECs should be increased for more strongly tidal systems where ice forms. It is clear, however, that larger machines are required for bigger tides.

No evidence has been found for large ice cakes that are near neutrally buoyant. Considering the set of mechanisms that might produce such ice cakes and transport them into Minas Passage, it seems that Sanders [6] overstates the danger that they pose to TISECs.

A search for subsurface drifting objects should be undertaken with the use of upwards looking sonar (bottom mounted) at proposed TISEC sites. We have also indicated how observations of ice cakes stranded low in the intertidal zone at low tide might be used to quantify the probability of subsurface ice cakes.

Acknowledgements

Jeremy E. Broome and Colin Buhariwalla assisted in the field. We thank Bruce MacDonald and Richard Clark for early discussion on ice cakes in Minas Basin. Funding was provided by the Nova Scotia Offshore Energy and Environmental Research Association.

References

[1] IPCC Fourth Assessment Report (AR4), Climate Change, 2007: Synthesis Report. <www.ipcc.ch/publications_and_data/publications_ipcc_fourth_assessment_report_synthesis_report.htm>.
[2] C.J. Campbell, The Coming Oil Crisis, Multi-Science Publishing Company & Petroconsultants, 1997.
[3] M.J. Dadswell, R.A. Rulifson, G.R. Daborn, Potential impact of large-scale tidal power developments in the upper Bay of Fundy on fisheries resources of the northwest Atlantic, Fisheries 11 (4) (1986) 26–35.
[4] R.H. Karsten, J.M. McMillan, M.J. Lickley, R.D. Haynes, Assessment of tidal current energy in the Minas Passage, Bay of Fundy, J. Power Energy 222 (2007) 493–507, http://dx.doi.org/10.1243/09576509JPE555.
[5] FORCE, Fundy Ocean Research Center for Energy Annual Report 2011, 2012. <www.fundyforce.ca/wp-content/uploads/2012/05/2011-FORCE-Annual-Report.pdf>.
[6] R. Sanders, Marine ice and other issues during harvest of tidal electricity from Nova Scotia's Minas Passage in 2011, J. Ocean Technol. 6 (2011) 34–56.
[7] C. Desplanque, D.I. Bray, Winter ice regime in the tidal estuaries of the northeastern portion of the Bay of Fundy, New Brunswick, Can. J. Civ. Eng. 13 (1986) 130–139.
[8] C. Lyell, Principles of Geology 1, John Murray, London, 1830.
[9] H.Y. Hind, The ice phenomena and the tides of the Bay of Fundy, considered in connection with the construction of Baie Verte Canal, Can. Mon. Nat. Rev. 8 (1875) 189–203.
[10] C. Desplanque, D.J. Mossman, A review of ice and tide observations in the Bay of Fundy, Atlantic Geol. 34 (1998) 195–209.
[11] H. Ridderinkhof, J.T.F. Zimmerman, Chaotic stirring in a tidal system, Science 258 (5085) (1992) 1107–1111, http://dx.doi.org/10.1126/science.258.5085.1107.
[12] Envirosphere, Oceanographic survey, oceanographic measurements—salinity, temperature & turbidity, Minas Passage Study Site August 2008–March 2009. A report submitted to: Minas Basin Pulp and Power Co. Ltd. By Envirosphere Consultants Limited, Windsor, Nova Scotia, 2009. <http://fundyforce.ca/wp-content/uploads/2012/05/G-Turbidity-Salinity-Temperature-EAA.pdf>.
[13] Oceans, Current in Minas Basin May 1, 2008–March 29, 2009 Submitted To: Minas Basin Pulp and Power. By: Oceans Ltd, 2009. <www.novascotia.ca/nse/ea/minas.passage.tidal.demonstration/Minas_EA_Vol_II_Appendix.05.pdf>.
[14] G. Neumann, W.J. Pierson, Principles of Physical Oceanography, Prentice-Hall, Englewood Cliffs, NJ, 1966.
[15] M. Black, Ebenezer Bishop, Kings County Vignettes, vol. 3, Published by Kings County Historical Society of Nova Scotia, 1965.
[16] C.A. Black, Geometry and composition of ice banks in a macrotidal channel (M.Sc. thesis), Department of Ocenography, Dalhousie University, Halifax, Nova Scotia, 2013.
[17] D. van Proosdij, J. Ollerhead, R.G.D. Davidson-Arnott, L. Schostak, Allen creek marsh, Bay of Fundy: a macro-tidal coastal saltmarsh, Can. Geogr. 43 (1999) 316–322.
[18] D.C.J. Gordon, C. Desplanque, Dynamics and environmental effects of ice in the Cumberland Basin of the Bay of Fundy, Can. J. Fish. Aquat. Sci. 40 (1983) 1331–1342.
[19] G.W. Timco, R.M.W. Frederking, A review of sea ice density, Cold Reg. Sci. Technol. 24 (1996) 1–6.
[20] A.E. Gill, Atmosphere-Ocean Dynamics, Academic Press, 1982.
[21] H. Tennekes, J.L. Lumley, A First Course in Turbulence, The MIT Press, Cambridge, 1972.
[22] K. Smith, J. Woods, A. Long, W.B. MacDonald, G. Fader, R. Bishop, S. Melrose, The characterization and tracking of sediment-laden ice in Minas Basin, Nova Scotia, in: A.M. Redden, J.A. Percy, P.G. Wells, S.J. Rolston (Eds.), Resource Development and its Implications in the Bay of Fundy and Gulf of Maine, Proceedings of the 8th BoFEP Bay of Fundy Science Workshop, Acadia University, Wolfville, Nova Scotia, May 26–29th 2009. Bay of Fundy Ecosystem Partnership Technical Report No. 4. Bay of Fundy Ecosystem Partnership, Wolfville, NS, 2009, pp. 63–74. <www.bofep.org/PDFfiles/BoFEP8thproceedings.pdf>.
[23] B.G. Sanderson, A. Okubo, I.T. Webster, S. Kioroglou, R. Appeldoorn, Observations and idealized models of dispersion on the soutwestern Puerto Rican insular shelf, Math. Comput. Modell. 21 (1995) 39–63.
[24] G.D. Brin, The "Great Silence": the controversy concerning extraterrestrial intelligent life, Q. J. R. Astron. Soc. 24 (1983) 283–309.

[25] G.S. Collins, H.J. Melosh, B.A. Ivanov, Modelling damage and deformation in impact simulations, Meteorit. Planet. Sci. 39 (2004) 217–231.
[26] G.W. Timco, M.E. Johnston, Sea ice strength during the melt season, in: Ice in the Environment: Proceedings of the 16th IAHR International Symposium on Ice, Dunedin, New Zealand, December 2nd–6th, 2002, International Association of Hydraulic Engineering and Research, 2002. <www.riverice.ualberta.ca/IAHR Proc/16th Ice Symp Dunedin 2002/Volume 2/148.pdf>.
[27] L.B. Tremblay, M. Hakakian, Estimating the sea ice compressive strength from satellite-derived sea ice drift and NCEP reanalysis data, J. Phys. Oceanogr. 36 (2006) 2165–2172.